International Journal of Mining Science and Technology 30 (2020) 859–864

Contents lists available at ScienceDirect

International Journal of Mining Science and Technology

journal homepage: www.elsevier.com/locate/ijmst

Effect of slurry conditioning on flocculant-aided filtration of coal tailings studied by low-field nuclear magnetic resonance and X-ray micro-tomography

Pengfei Hu [a,b], Long Liang [a,b,*], Guangyuan Xie [a,b], Shaoqi Zhou [a,b], Yaoli Peng [a,b]

[a] Key Laboratory of Coal Processing and Efficient Utilization of Ministry of Education, China University of Mining and Technology, Xuzhou 221116, China
[b] School of Chemical Engineering and Technology, China University of Mining and Technology, Xuzhou 221116, China

ARTICLE INFO

Article history:
Received 3 May 2020
Received in revised form 15 June 2020
Accepted 29 July 2020
Available online 8 August 2020

Keywords:
Coal tailings
Filtration
Slurry conditioning
Nuclear magnetic resonance
X-ray micro-tomography

ABSTRACT

The present work aimed to study the effect of slurry conditioning on flocculant-aided filtration of coal tailings by the analysis of filtration kinetics and filter cake structure. Laboratory filtration tests of the coal tailings showed that both the shear rate and agitation time have significant effects on filtration rate and cake moisture. Moderate agitation at the shear rate of 92 s^{-1} was favorable for fast filtration, but high cake moisture was encountered. The low-field ^{1}H nuclear magnetic resonance (NMR) measurements of the filter cake showed that the slurry conditioning has a significant effect on the residual water in large pores and a negligible effect on the residual water in small pores. The X-ray micro-tomography (XRM) measurements indicated that the filter cake formed at the shear rate of 92 s^{-1} has more macro-pores and higher porosity than that formed at the shear rate of 53 s^{-1}, hence more residual water was entrapped in filter cake. The slurry conditioning in the presence of flocculant will change the structure of filter cake and affect the filtration performance. There was a paradox between fast filtration rate and low filter cake moisture. The findings enable better understanding of the effect of slurry conditioning on flocculant-aided filtration of coal tailings.

1. Introduction

Filtration is an important solid–liquid separation process that can be applied in various fields such as industrial water recycling, sewage sludge treatment, and papermaking wastewater separation [1–5]. Filtration of coal slurry is essential in coal preparation plant because the fresh water is precious resource and must be recycled. On the other hand, high moisture of filter cake needs to be avoided because it can reduce the calorific value and increase the transportation cost [6,7]. Compared to the clean coal, fast filtration of coal tailings is difficult to achieve due to the presence of clay minerals and the high slurry viscosity [8]. In order to improve the filtration efficiency, flocculants are usually added in coal tailings to destabilize the fine particles and agglomerate them into flocs. Alam et al. [9] studied the effect of preconditioning of coal tailings with varying flocculants at different dosages, and they found that the optimum flocculant addition regime for efficient filtration is to add anionic flocculant at 350 g/t at 35% solid concentration. Tao et al. [10] studied the filtration kinetics of ultrafine coal with the addition of cationic and anionic flocculants, and the results showed that flocculation reduces the resistance of water flow in filter cake and renders the filtration rate less dependent on the filtration driving force.

Most of the previous research concerned the application of flocculant in fine coal filtration was concentrated on the type and dosage of flocculant. Slurry conditioning attained less attention although it plays an important role in filtration efficiency. Ofori et al. [11] studied the application of shear-induced structural changes in flocs to improve dewatering efficiency of coal tailings, and the results showed that large flocs form at low mixing speeds, and a high settling rate is obtained, while irreversible floc degradation and a much reduced settling rate with additional sediment consolidation occur at very high mixing speed. Although the slurry conditioning is a key factor to bring the flocculant into full play, scarce information is available in literature regarding the effect of slurry conditioning on flocculant-aided filtration performance.

There are diverse methods of characterizing the filtration process and filter cake structure. Fan et al. [8] and Alam et al. [9] developed specially designed filtration apparatuses to determine

* Corresponding author.
E-mail address: lianglong1218@sina.com (L. Liang).

https://doi.org/10.1016/j.ijmst.2020.07.008
2095-2686/

the filtration rate, residual moisture, and resistance of filter cake simultaneously. The laser particle size analyzer and turbidimeter are frequently used to characterize the flocculation efficiency when flocculant is added to accelerate filtration [12]. The scanning electron microscope (SEM) can characterize the porosity and structure of filter cake, but it is not easy to get quantitative results. Low-field nuclear magnetic resonance (NMR) is a nondestructive and rapid technique of measuring the distribution of water embedded in solids [13–15]. Kim et al. [16] reported the distribution of water in Loy Yang brown coal measured by solid-state ^{1}H NMR. Zhang et al. [17] characterized the water imbibition process in sandstones using NMR technique, and the results were verified by the weighing method. The application of low-field NMR in measuring water distribution can also be found in meat batters [18]. The X-ray micro-tomography (XRM) is a powerful tool to characterize the microstructure and space distribution of pores in solid materials such as electrode [19], cement paste [20], and coal [21]. It is also applicable to characterize the distribution of pores in filter cake, but scarce application of XRM in coal filtration is available in literature.

The present work aimed to achieve better understanding of the effect of slurry conditioning on filtration performance of coal tailings. To analyze the distribution of residual water in filter cake, the NMR measurement of the filter cake was conducted. In addition, the state of water in filter cake was classified according to the drying rate curve coupled with the determination of the cutoff value of transverse relaxation time. The three-dimensional XRM measurements of the filter cake were also conducted to validate the results obtained by NMR.

2. Material and methods

2.1. Materials

The coal tailings slurry used in this study was from a coal preparation plant in Jincheng, Shanxi Province, China. Fig. 1 shows the weight and ash content distributions of different particle size fractions of the coal tailings. It is obvious from Fig. 1 that the weight and ash content of the coal of –45 μm size fraction were higher than that in other size fractions, indicating a high proportion of clay minerals in the coal tailings. The pH value of the slurry is 8.6. The concentrations of major ions in the process water assayed by Inductively Coupled Plasma Mass Spectrometry (NWR 213–7900 ICP-MS, Agilent) are listed in Table 1.

The flocculant used in this study was anionic polyacrylamide (PAM) with a molecular weight of 10000 kg/mol and a charge density of 30%, purchased from Sinopharm Co., Ltd. The PAM was stirred in the deionized (DI) water of a resistivity 18.2 MΩ·cm (Canrex Analytic Instrument Ltd., China) at 400 rpm at room temperature for 60 min using a magnetic agitator to dissolve the PAM powder and prepare a solution at 0.3 wt% before use.

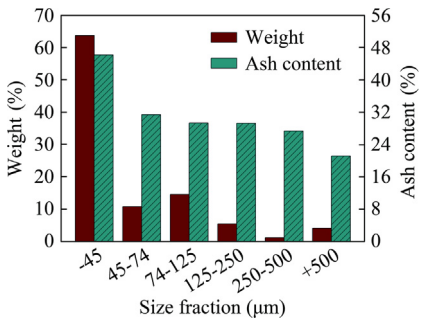

Fig. 1. Distribution of weight and ash content in different size fractions of coal tailings.

Table 1
Concentrations of major ions in the process water.

Element	Concentration (mg/L)
Na^{+}	3107.45
Mg^{2+}	429.02
Ca^{2+}	167.64
K^{+}	125.69
SO_4^{2-}	3924.21
Cl^{-}	1536.23

2.2. Filtration experiments

The filtration experiments were carried out using the apparatus shown in Fig. 2. The coal tailings slurry of 80 mL in a beaker (6.5 cm diameter) of 200 mL was mixed with PAM solution at 200 g/t dosage, i.e. 2.7 mL of the PAM solution was added in the slurry. Then the coal tailings with pulp density of 500 g/L were stirred at a predetermined speed (100, 200, 300, and 500 rpm) and time (30, 60, 90, and 120 s) by an adjustable speed mixer (JB90-S, Shanghai Precision instrument Ltd., China) with a three bladed impeller of 4.0 cm diameter. In the experiments in the absence of PAM, DI water of 2.7 mL was added in the beaker to keep the solid concentration consistent. After the conditioning, the slurry was poured into the Buchner funnel and the vacuum pump was then switched on to start the filtration. During the filtration, the filtrate was allowed to drop into the measuring cylinder in the vacuum flask at a vacuum pressure of 0.1 MPa. The vacuum flask and measuring cylinder were made of transparent glass, therefore the volume of the filtrate could be read and recorded over time.

2.3. Low-field nuclear magnetic resonance (NMR) measurements

In measuring the residual water in filter cake, the magnet of the NMR instrument generates a magnetic field. The magnetic field can activate the protons in the water molecules present in the NMR probe because the hydrogen atom in water has a high gyromagnetic ratio. Subsequently, the oscillating field is removed and the protons begin to relax towards the original direction in which the static magnetic field aligns them. The time constant of the transverse magnetization decay is called the transverse relaxation time (referred to as T_2). Therefore, the distribution of T_2 can assess the intensity of hydrogen protons in water, indicating the distribution of residual water in filter cake.

In the present study, the NMR measurements were conducted using NMRC12-010 V, Niumag, China, at resonant frequency of 12.5 MHz, and the magnet temperature was fixed to 32 °C. The Carr-Purcell-Meiboom-Gill (CPMG) sequence was used to test T_2 spectra. The other detailed operating parameters are presented in Table 2. In each test, the sample of 7 g taken from the center of

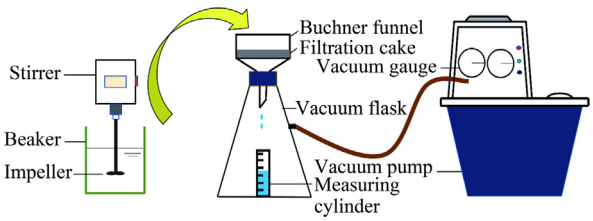

Fig. 2. The apparatus of laboratory filtration test.

Table 2
Operating conditions for the NMR measurements.

Parameter	Value
90° pulse width (μs)	5.0
180° pulse width (μs)	9.0
Wait time (ms)	3000
Number of echoes	4096

the filter cake was put into the NMR tube and was sealed to prevent water loss during the experiment.

2.4. Drying kinetics of the filter cake

The filter cake was dried in an opened weighing bottle in an oven at 110 °C. The bottle was taken out from the oven and weighed every a few minutes to determine the moisture. In order to avoid the temperature drop when the oven was opened, a fast heating-up oven (XCQ-2000, Hongci Machinery) was used. The drying rate curve was plotted according to the weight loss rate and the corresponding moisture content, and the critical points on the drying rate curve were used to classify the state of water. The detailed description of this method could be found in the work of Kim et al. [16] and Allardice & Evans [22]. In the determination of T_2 cutoff value, the oven drying rate test was repeated under the same conditions after the critical points were confirmed and the test was stopped when the filter cake had been dried for the corresponding moisture content of the critical points.

2.5. X-ray micro-tomography (XRM) analysis

The internal structure analysis of the filter cake was studied using the high solution three-dimensional X-ray micro-tomography (Xradia 520 Versa, Zeiss) with the highest spatial resolution of 5 μm. The measurement sample was a cylinder of 5 mm in diameter obtained from the center of the filter cake using a hollow plastic pipe. When X-ray passed through the rotating sample, the two-dimensional projected images of the filter cake slices at different angles were obtained. Then, the digital geometry processing technology was used to reconstruct a three-dimensional image of internal structure of the filter cake. The distribution of pores and the porosity of filter cake were analyzed using a commercial software Dragonfly.

3. Results and discussion

3.1. Filtration experiments

Fig. 3a and b show the variation of filtrate volume as a function of filtration time at different shear rates and agitation time, respectively. In order to present the experimental law concisely, four conditions of shear rate and agitation time were respectively selected in a series of laboratory exploration experiments. As seen in Fig. 3, the filtration rate and the ultimate filtrate volume varied under different conditions. According to the dramatic changes in curvature, the filtration process could be divided into two stages, namely the cake formation stage and the cake dewatering stage [10]. In general, the faster the filtration rate in the cake formation stage, the lower the ultimate filtrate volume would be, indicating a higher moisture content of the filter cake. In order to analyze quantitatively the tendency, the curves were fitted with the classical first order model as shown in Eq. (1).

$$\varepsilon = \varepsilon_\infty(1 - \exp(-kt)) \tag{1}$$

where ε is the filtrate volume in mL at time t; ε_∞ the ultimate filtrate volume in mL; k the filtration rate constant in s^{-1}; and t the filtration time in s. The ultimate filtrate volume (ε_∞) and the filtration rate constant (k) were plotted as a function of shear rate and agitation time, as shown in Fig. 4a and b, respectively. The error bars in Fig. 4 represent one standard deviation obtained from three independent tests.

Fig. 3a and Fig. 4a show that shear rate has significant effects on both filtration rate and ultimate filtrate volume. As the shear rate increased from 53 to 92 s^{-1}, the filtration rate increased while the ultimate filtrate volume decreased. As the shear rate further increased to 185 s^{-1}, the filtration rate steadily decreased but the filtrate volume increased. It took 35 s for the filter cake to attain a moisture content of 28.6% for the coal tailings agitated with a shear rate of 92 s^{-1}, and took more than 40 s for that agitated with other shear rates. This means that the agitation with moderate shear rate (e.g. 92 s^{-1}) was favorable for fast filtration, but it was not beneficial to reduce the filter cake moisture. The agitation with mild or extensive shear rate would be appropriate if low filter cake moisture was desirable and the fast filtration rate was not neces-

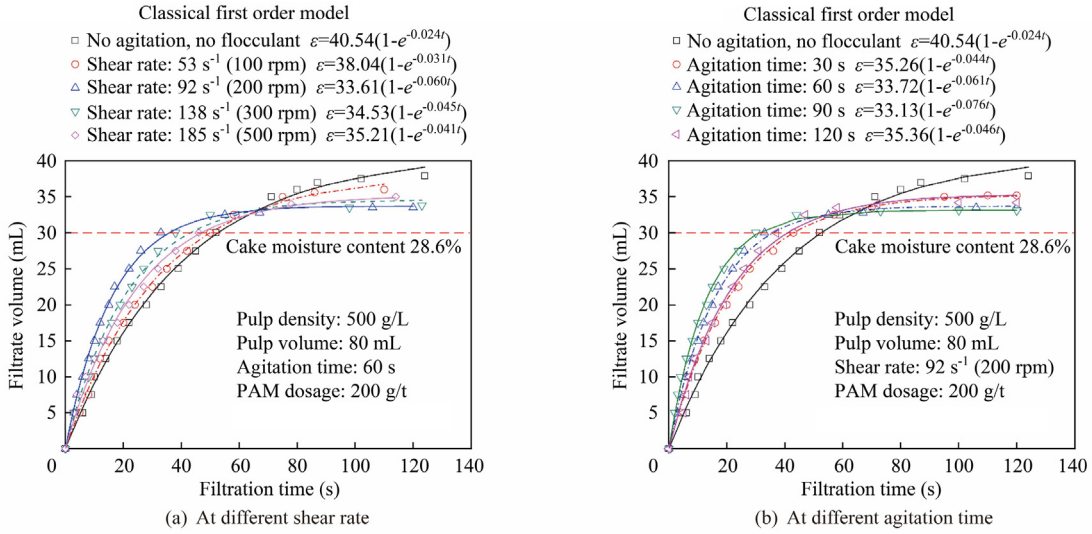

Fig. 3. The variation of filtrate volume versus time for coal tailings agitated at different shear rate and agitation time.

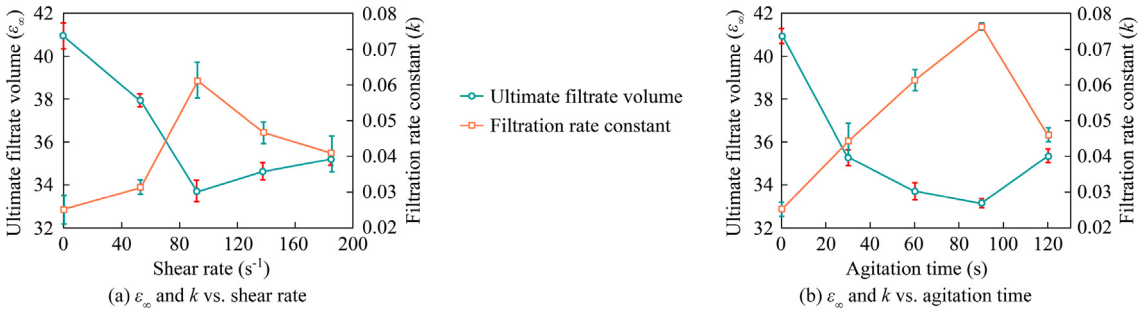

Fig. 4. The ultimate filtrate volume and filtration rate constant as a function of shear rate and agitation time.

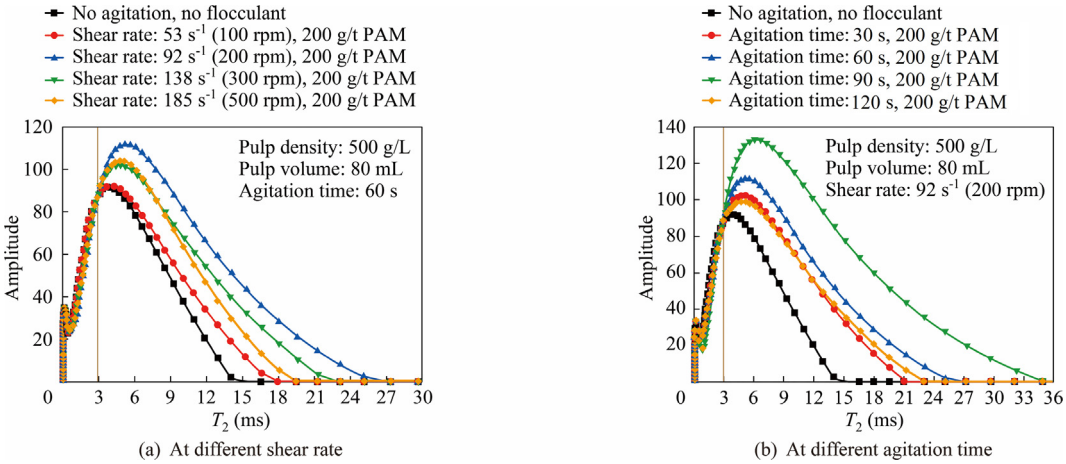

Fig. 5. T_2 spectra for filter cake obtained from the coal tailings agitated at different shear rate and agitation time.

sary. Fig. 3b and Fig. 4b show that agitation time also has significant effects on both the filtration rate and ultimate filtrate volume. As the agitation time increased, the filtration rate increased to a plateau of 0.075 s^{-1} at the agitation time of 90 s and then decreased, while the variation of filter volume, on the contrary, decreased to a valley of 33 mL at the agitation time of 90 s and then increased.

Researchers proposed that there does not exist a microstructure that is capable of providing both a high filtration rate and a low product moisture at the same time [23]. This is because large aggregates are desirable for fast filtration in the cake formation stage, however, large aggregates with loose structure would cause more water entrapped in filter cake. The results of filtration experiments suggest that a mild shear rate and too short agitation time was not conducive to forming aggregates and the effect of flocculant on increasing filtration rate would be diminished. Meanwhile, an extensive shear rate or too long agitation time might break the aggregates into small ones, resulting in a low filtration rate.

3.2. NMR measurements of the filter cake

The NMR measurements were performed for the filter cakes obtained in the filtration experiments, and the results are shown in Fig. 5. To highlight the difference in T_2 distribution, the ordinary abscissa was used instead of the commonly used logarithmic abscissa. It is obvious from Fig. 5 that the difference in the distribution of $0 < T_2 < 3$ ms was negligible, however, the difference became significant for T_2 greater than 3 ms. The amplitude of T_2 distribution and the maximum T_2 value in the absence of flocculant were both the smallest. As shown in Fig. 5a, the largest T_2 value was obtained for filter cake at the shear rate of 92 s^{-1}, followed by 138, 185, and 53 s^{-1}, which was consistent with the variation trend of the ultimate filtrate volume in Fig. 4a. Fig. 5b shows that the largest T_2 value was obtained for the filter cake after the slurry was agitated for 90 s, followed by that of 60, 120, and 30 s, which was also consistent with the variation trend of the ultimate filtrate volume in Fig. 4b. The similar consistency could also be found in the amplitude of T_2 distribution. The results indicate that the NMR results can reflect the filter cake moisture, and the slurry conditioning has a significant effect on the distribution of T_2 greater than 3 ms and a negligible effect on the distribution of $0 < T_2 < 3$ ms. The meaning of $T_2 = 3$ ms needs further interpretations.

3.3. Classification of the state of water in NMR T_2 spectrum

The water embedded in coal can be classified into four states, i.e. the free water, the interstitial water, the surface water, and the hydration (or internal) water. The free water refers to the water in the voids of coal particles and would be unaffected by the capillary force. The sum of the three latter states of water is usually collectively called the bound water [24–26].

Fig. 6 shows the drying rate curves of the filter cakes for water classification. It can be found that the drying rate of the filter cakes obtained under different conditions decreased with the decrease of moisture content. Two critical points of the moisture content were appointed in Fig. 6 (marked with red circles) according to the saltation of the drying rate curve. After the 1st critical point, the free water in the filter cake was considered to be completely removed [16]. It is worth noting that the critical points on the two drying

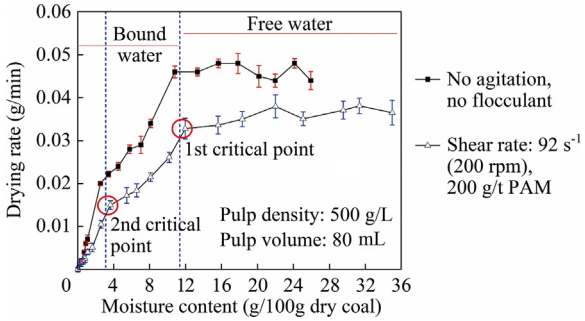

Fig. 6. The drying rate curve of the filter cake.

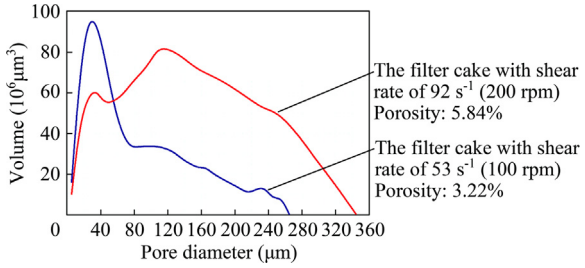

Fig. 8. Pore size distribution in filter cake extracted from the XRM datasets.

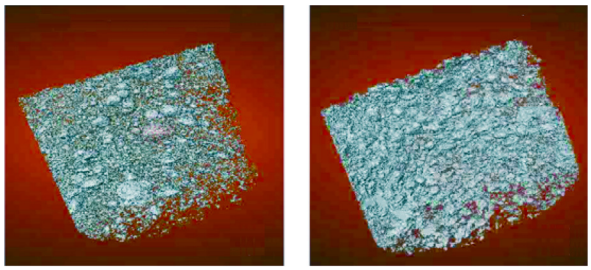

(a) At the shear rate of 53 s-1 (100 rpm)

(b) At the shear rate of 92 s-1 (200 rpm)

Fig. 9. Three-dimensional XRM image of filter cake pores.

rate curves corresponded to similar moisture contents, in spite of the difference larger than 9% in the initial moisture content of the two filter cakes. In other words, the difference in the moisture content contributed by free water between the two cakes was large, while the moisture content contributed by water in other states was similar. Combined with the NMR results, it can be speculated that the residual water that was significantly affected by slurry conditioning was possibly the free water.

The T_2 cutoff value (T_{2c}) was used to classify the different states of water in T_2 spectrum. The process for determining T_{2c} and classifying the water state in filter cake can be found in the work of Yao et al. [27] and Westphal et al. [28], as briefly illustrated in Fig. 7. T_2 distributions of two filter cakes were plotted. One is denoted as C_o, corresponding to the original filter cake after the agitation of coal tailings at the shear rate of 92 s^{-1}. And the other is denoted as C_d, corresponding to the same filter cake that had been oven dried to the 1st critical point, that is, the free water had been removed. The NMR T_2 distributions of the these two filter cakes were transformed into two accumulative T_2 spectra. Then, the curve was projected horizontally from the top of the accumulative curve of the filter cake C_d to the accumulative curve of the filter cake C_o. Finally, the T_2 value corresponding to the intersection on the T_2 axis was confirmed to be the T_2 cutoff value (T_{2c}), which was 3 ms in the present work. It was confirmed that the T_2 value exceeding 3 ms corresponded to the free water in the filter cake, indicating that the slurry conditioning mainly affected the free water in filter cake but did not affect the bound water.

3.4. XRM analysis of the filter cake

The image segmentation of the pores of filter cake in XRM dataset was performed using the Dragonfly software. The pore size distributions in filter cakes extracted from the XRM datasets are shown in Fig. 8. According to the spatial resolution, the pores larger than 5 μm in diameter were analyzed. As shown in Fig. 8, the porosities of the filter cake at the shear rate of 53 and 92 s^{-1} were 3.22% and 5.84%, respectively. For pore diameter smaller than 60 μm, both curves attained a plateau at around 30 μm, and the filter cake at shear rate of 53 s^{-1} had a large volume than that at shear rate of 92 s^{-1} in this pore diameter range. On the contrary, the pore volume of the filter cake at the shear rate of 92 s^{-1} was larger than that at the shear rate of 53 s^{-1} for pore diameter larger than 60 μm. It is evident that the filter cake obtained from moderate agitation (92 s^{-1}) had a higher porosity than that obtained from mild agitation (53 s^{-1}), and the former had significantly more macropores. The difference between the pore structures in the two filter cakes can also be seen in the three-dimensional XRM images (Fig. 9). These results are consistent with the results of filtration experiments in Fig. 4.

The flocculant molecules acted as bridges that connected the coal particles in slurry to form flocs, and the floc size was significantly dependent on slurry conditioning. The larger the flocs, the faster the free water that accumulated between the flocs could be filtrated. However, the larger flocs entrapped more free water in the macro-pores in filter cake, causing the higher moisture. The particle surface properties such as surface charges and hydrophilicity/hydrophobicity can affect the bound water either by electrostatic means or via hydrogen bonds [29,30]. Therefore, it can be inferred from the stable bound water that agitation did not change the particle surface characteristics.

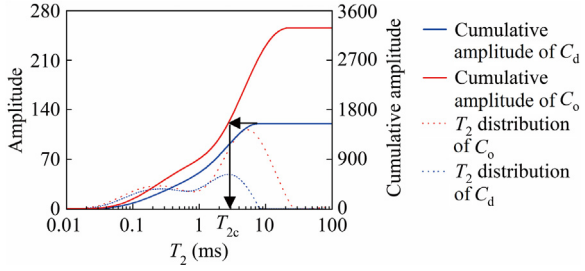

Fig. 7. T_2 cutoff value (T_{2c}) from the T_2 distributions of the filter cake C_o and the filter cake C_d.

4. Conclusions

The effect of slurry conditioning on the filtration of coal tailings was investigated in this study. The filtration results indicated that the slurry conditioning significantly affects the filtration rate and the residual moisture in filter cake. The moderate agitation at the shear rate of 92 s^{-1} was favorable for fast filtration, but high residual water in filter cake was encountered.

The NMR measurements indicated that the T_2 distribution can reflect the distribution of residual moisture in filter cake. The slurry conditioning had a significant effect on the residual water in relatively large pores (T_2 greater than 3 ms). A combination of

drying rate curve and T_2 cutoff value determination classified the state of water in NMR T_2 spectrum. It was confirmed that T_2 greater than 3 ms corresponded to the free water in filter cake while $0 < T_2 < 3$ ms corresponded to the bound water in filter cake.

The XRM measurements of the micron-scale pore distribution in filter cake showed that the filter cake formed at shear rate of 92 s^{-1} has a higher porosity than that formed at shear rate of 53 s^{-1}. Meanwhile, the former contained more macropores larger than 60 μm, hence more free water was entrapped in the pores in filter cake.

This study showed that the slurry conditioning plays an important role in the flocculant-aided filtration of coal tailings. It is difficult to form a filter cake structure that can provide both a high filtration rate and a low product moisture. These findings should be taken into consideration to obtain the desired filtration performance.

Acknowledgements

This work was supported by the Natural Science Foundation of Jiangsu Province (BK20180657). The authors would also like to express thankfulness to the Priority Academic Program Development of Jiangsu Higher Education Institutions.

References

[1] He D, Wang L, Jiang H, Yu H. A Fenton-like process for the enhanced activated sludge dewatering. Chem Eng J 2015;272:128–34.
[2] Mo R, Huang S, Dai W, Liang J, Sun S. A rapid Fenton treatment technique for sewage sludge dewatering. Chem Eng J 2015;269:391–8.
[3] Meng J, Yin F, Li S, Zhong R, Sheng Z, Nie B. Effect of different concentrations of surfactant on the wettability of coal by molecular dynamics simulation. Int J Min Sci Technol 2019;29(4):577–84.
[4] Qi Y, Thapa KB, Hoadley AFA. Application of filtration aids for improving sludge dewatering properties - A review. Chem Eng J 2011;171:373–84.
[5] Dai Z, Shi L, Wang L, Guo C. Rheological behaviors of coal slime produced by filter-pressing. Int J Min Sci Technol 2018;28(2):347–51.
[6] Tao D, Groppo JG, Parekh BK. Enhanced ultrafine coal dewatering using flocculation filtration processes. Miner Eng 2000;13:163–71.
[7] Gong G, Xie G, Zhang Y, Wang Z, Wang J, Xie L, et al. Effect of a starch-based filter aid on the dewatering of fine clean coal. Mining Science and Technology 2010;20:635–40.
[8] Qin Z. New advances in coal structure model. Int J Min Sci Technol 2018;28(4):541–59.
[9] Dwari RK, Mishra BK. Evaluation of flocculation characteristics of kaolinite dispersion system using guar gum: A green flocculant. Int J Min Sci Technol 2019;29(5):745–55.
[10] Tao D, Parekh BK, Liu JT, Chen S. An investigation on dewatering kinetics of ultrafine coal. Int J Miner Process 2003;70:235–49.
[11] Ofori P, Nguyen AV, Firth B, McNally C, Ozdemir O. Shear-induced floc structure changes for enhanced dewatering of coal preparation plant tailings. Chem Eng J 2011;172:914–23.
[12] Eskibalci MF, Ozkan MF. Comparison of conventional coagulation and electrocoagulation methods for dewatering of coal preparation plant. Miner Eng 2018;122:106–12.
[13] Yao Y, Liu D, Liu J, Xie S. Assessing the Water Migration and Permeability of Large Intact Bituminous and Anthracite Coals Using NMR Relaxation Spectrometry. Transp Porous Media 2015;107:527–42.
[14] Sun X, Yao Y, Liu D, Zhou Y. Investigations of CO_2-water wettability of coal: NMR relaxation method. Int J Coal Geol 2018;188:38–50.
[15] Zhao Y, Sun Y, Liu S, Wang K, Jiang Y. Pore structure characterization of coal by NMR cryoporometry. Fuel 2017;190:359–69.
[16] Kim H-S, Nishiyama Y, Ideta K, Miyawaki J, Matsushita Y, Park J-I, et al. Analysis of water in Loy Yang brown coal using solid-state ^{1}H NMR. J Ind Eng Chem 2013;19:1673–9.
[17] Zhang Q, Dong YH, Tong SQ. Characterization of water imbibition in sandstones studied using nuclear magnetic resonance. Journal of University of Chinese Academy of Sciences 2017;34:610–7.
[18] Shao JH, Deng YM, Jia N, Li RR, Cao JX, Liu DY, et al. Low-field NMR determination of water distribution in meat batters with NaCl and polyphosphate addition. Food Chem 2016;200:308–14.
[19] Taiwo OO, Finegan DP, Gelb J, Holzner C, Brett DJL, Shearing PR. The use of contrast enhancement techniques in X-ray imaging of lithium-ion battery electrodes. Chem Eng Sci 2016;154:27–33.
[20] Jeong SB, Yokota M, Kawasaki S, Kim BK, Kaneko K, Cho SH, et al. Electrical disintegration and micro-focus X-ray CT observations of cement paste samples with dispersed mineral particles. Miner Eng 2014;57:79–85.
[21] Zhang X, Lin B, Li Y, Zhu C, Kong J, Li Y. Enhancement effect of NaCl solution on pore structure of coal with high- voltage electrical pulse treatment. Fuel 2019;235:744–52.
[22] Allardice DJ, Evans DG. The-brown coal/water system: Part 2. Water sorption isotherms on bed-moist Yallourn brown coal. Fuel 1971;50:236–53.
[23] Lemanowicz M, Jach Z, Kilian E, Gierczycki A. Ultra-fine coal flocculation using dual-polymer systems of ultrasonically conditioned and unmodified flocculant. Chem Eng J 2011;168:159–69.
[24] Wei H, Gao B, Ren J, Li A, Yang H. Coagulation/flocculation in dewatering of sludge: a review. Water Res 2018;143:608–31.
[25] Rao Z, Zhao Y, Huang C, Duan C, He J. Recent developments in drying and dewatering for low rank coals. Prog Energy Combust Sci 2015;46:1–11.
[26] Du Hong Y, Lin BQ, Zhu CJ, Li H. Effect of microwave irradiation on petrophysical characterization of coals. Appl Therm Eng 2016;102:1109–25.
[27] Yao Y, Liu D, Che Y, Tang D, Tang S, Huang W. Petrophysical characterization of coals by low-field nuclear magnetic resonance (NMR). Fuel 2010;89:1371–80.
[28] Westphal H, Surholt I, Kiesl C, Thern HF, Kruspe T. NMR measurements in carbonate rocks: Problems and an approach to a solution. Pure Appl Geophys 2005;162:549–70.
[29] Vaxelaire J, Cézac P. Moisture distribution in activated sludges: A review. Water Res 2004;38:2215–30.
[30] Nasser MS, James AE. The effect of polyacrylamide charge density and molecular weight on the flocculation and sedimentation behaviour of kaolinite suspensions. Sep Purif Technol 2006;52:241–52.